

# Extensive Study on 3d Scanning Technology in Product Development and Suspension System Advancements

P. V. Gopal krisha<sup>1</sup> S. Madhava sai<sup>2</sup>

1. Associate Professor, 2. PG student, Department of Mechanical Engineering,  
Vasavi College of Engineering, Hyderabad, Telangana, India

---

## ARTICLE INFO

Received: 30 Dec 2024

Revised: 12 Feb 2025

Accepted: 26 Feb 2025

## ABSTRACT

This study introduces an innovative methodology that leverages precise and cost-effective 3D scanning technology to facilitate seamless transitions between digital models and physical prototypes. The proposed approach significantly enhances both cost efficiency and effectiveness in product development. The implementation of this methodology led to a notable 28% reduction in material waste and time consumption during the redesign of a security camera mount. Iterative design enhancements achieved a 22% decrease in time consumption and improved alignment with customer requirements. For electric motorbike design, the use of 3D scanning technology enhanced the design validation process by 15%. In suspension design, advanced performance testing and material simulation resulted in a 30% reduction in production costs and a 20% increase in structural integrity. These results underscore the methodology's substantial impact on optimizing product development processes, offering practical solutions for industry professionals and providing valuable insights for future advancements.

## Keywords:

---

## 1. INTRODUCTION

In product development (PD) and industrial design, the integration of both physical and digital 3D models during early stages is standard practice for testing and refining designs. Despite advancements in 3D printing technology, which have reduced costs associated with creating intricate physical models, a persistent challenge remains in efficiently generating the required digital designs. Computer-aided design (CAD) tools equipped with freeform surface modelling capabilities and 3D scanning equipment are commonly used for developing digital models with complex shapes. However, these tools are considered high-investment due to time requirements for quality results and associated costs of equipment and software. In industrial design, early-phase physical models crafted from materials like clay, cardboard, or wood are crucial. They provide tangible experiences and spatial insights into interactions between products and users. These models allow for comprehensive exploration of aesthetic aspects such as tactile, visual, and ergonomic elements, which CAD alone cannot fully replicate. Material-driven design practices, involving prototypes made from natural materials such as wood and clay, emphasize preserving surface imperfections as integral to the final design. However, digitizing these models early in the design process remains a challenge.

Early-stage PD projects heavily rely on physical prototypes to provide valuable experiential feedback and support decision-making. Prototypes made from low-cost, high-uncertainty materials like cardboard and clay facilitate exploration of design solutions and identification of potential issues early on. Costly and time-intensive CAD models may hinder iterative design changes during these critical stages. Integrating 3D scanning methods, particularly low-cost options like photogrammetry using a single digital camera, addresses challenges in combining physical and digital prototyping early in the PD process. This approach enables the designing, building, and testing of complex and organic designs efficiently.

This study aims to prototype and evaluate the feasibility, considering effort, skill, and investment, of employing low-cost 3D scanning (photogrammetry) in early PD workflows. A proof-of-concept 3D scanning setup is described, and its applications are explored through two case studies: 1) Real-World Industrial Design Application: Digitization of

an electric vehicle (EV) scooter design, and 2) Experimental Prototyping: Custom-fit gear rod knob and security camera support. By bridging the gap from physical to digital and back to physical prototyping, this research seeks to uncover limitations of the method and provide insights for enhancing future PD activities and research .

## 2. 3D SCANNING METHOD, SETUP, AND PIPELINE

Photogrammetry finds applications across various domains, including the documentation of 3D cultural heritage, design of prosthetic sockets , utilization in geoscience, and measurement of car body deformation in the automotive sector . Despite being traditionally perceived as a complex and labour-intensive task reserved for experts , recent advancements and innovative techniques have streamlined the photogrammetry process. By employing photographs taken from different angles, photogrammetry algorithms, particularly Structure from Motion (SfM) and Multi View Stereo (MVS), can effortlessly generate 3D point clouds and meshes. One notable advantage of photogrammetry is its accessibility, as the increasing affordability of various 3D scanners, including time-of-flight, LiDAR, and structured light scanners, allows most individuals to have the necessary hardware. Moreover, only a digital camera and a computer are required, with several open-source implementations readily available for processing. Photogrammetry is characterized by the fact that there is no limit to the size of objects that can be scanned and does not require complex setups or calibrations to create high-quality 3D models. This feature makes it easy to customize and automate the entire process.

### 2.1 Algorithms of Open-source photogrammetry

The process of creating 3D digital models from photos begins with Structure from Motion (SfM). We examine unstructured photos of an item or scene, calculate camera locations, and generate a sparse point cloud using the open-source incremental SfM program COLMAP. We use Multi-View Stereo (MVS) methods to further refine this into a comprehensive mesh. Open MVS, which is effective for both small and large datasets (e.g., clay models), and COLMAP's MVS pipeline, which is appropriate for large and complicated datasets, are used. From the SfM output, MVS calculates normal and depth information for each pixel, merging them to create a dense point cloud. Next, a surface mesh is produced using the Poisson reconstruction method. Open MVS produces a textured mesh, whereas COLMAP produces a mesh with vertex colors. Command line automation is supported with both tools.

### 2.2 3D scanning provision

The 3D scanning system consists of four major components: a mobile camera, a picture booth, a turntable, and a processing laptop. Its purpose is to automate and simplify the scanning process. A OnePlus 5T phone, mounted on an adjustable arm and controlled via Bluetooth, is used in the arrangement. It has two cameras: a 16 MP,  $f/1.7$ , 27 mm (wide),  $1/2.8''$ ,  $1.12 \mu\text{m}$ , PDAF, and a 20 MP,  $f/1.7$ , 27 mm (wide),  $1/2.8$  inch,  $1.0 \mu\text{m}$ , AF, PDAF. To achieve the best possible image quality, the focus and camera settings are manually changed. Shadows are reduced in the photo booth by using matte black graph paper. The laptop handles scanning, 3D reconstruction, and post-processing with a 2.4 GHz 6-core Intel Core i5 CPU and an Nvidia GeForce GTX 1650Ti GPU. Scripts create timestamped documents and automate processes.

Table 1. Camera settings used for 3D scanning.

Setting	Value	Objective
f-number	Auto	Maintains subject detail (focus) while diffusing the background.
ISO	160	In good lighting, lower ISO values are possible and is used for noise reduction.
Shutter speed	1/38 seconds	A fast shutter speed is required to reduce or eliminate motion blur caused by the turntable continuing to rotate during recording.
Resolution	3456x4608	With regular JPEG quality and smaller image size, reduces processing time and file size over while providing sufficient detail.

### 2.3 Post processing process

Digital imaging and 3D printing usually require further post-processing, but scanned and reconstructed models are usually adequate. First use is frequently with MeshLab, an open-source program with a (GUI). Using scripting, it automates mesh editing operations such as color-based removal, hole closure, and net adjustment. The model is scaled in MeshLab by measuring known distances and then exported as an STL file for 3D printing. Models with thin

surfaces can be given more thickness using Autodesk Meshmixer. Advanced CAD integration and freeform surface modifications are provided by Siemens NX, and the model can be exported as a STEP file for manufacture. Slic3r Prusa Edition and Simplify3D software are used for FDM printing with PLA material, with a Prusa i3 MK3 for smaller prints and a 3DP Work Series 400 for bigger ones.

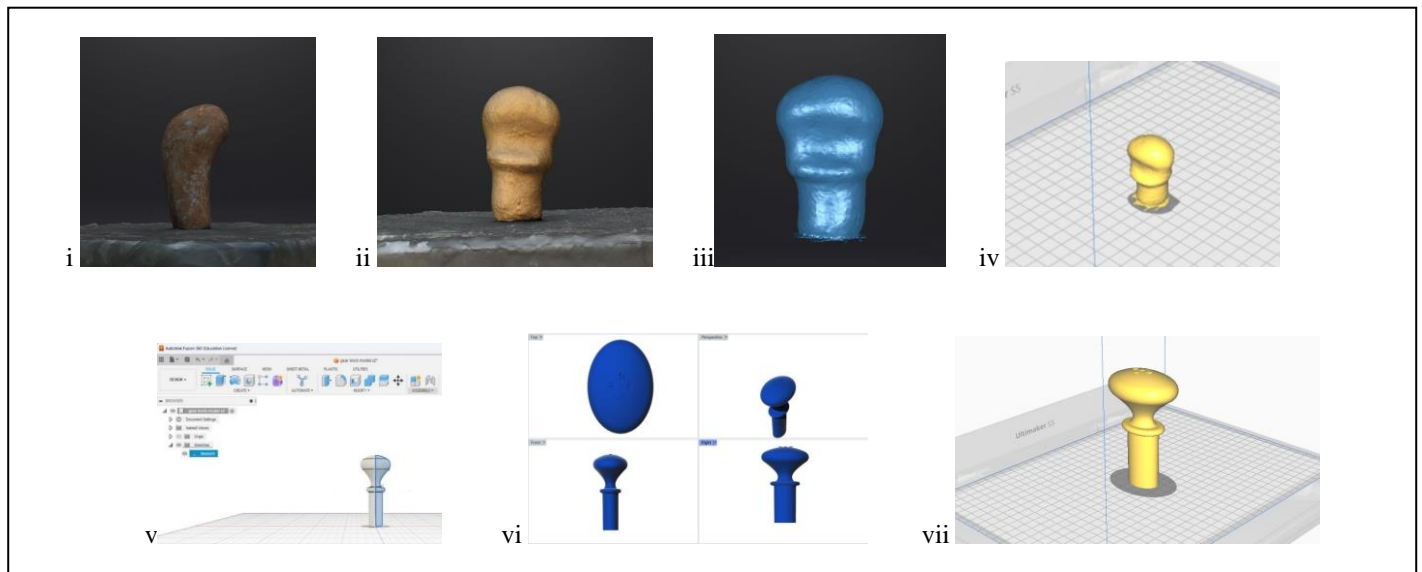
#### 2.4. Overview of the 3D scanning pipeline and limitations

Figure 2 presents an overview of the 3D scanning pipeline as a workflow diagram, covering stages from physical prototyping (e.g., creating a clay model) to generating and refining a digital representation, and then producing an enhanced physical prototype (e.g., using stronger materials or adding parametric features). Insights gained from new prototypes help improve the original design or explore new concepts. Photogrammetry faces key limitations: lack of texture, thin structures, and non-Lambertian surfaces. Uniform surfaces without texture are difficult to reconstruct because features cannot be triangulated. Thin structures that occupy few pixels are challenging for MVS algorithms, while non-Lambertian surfaces (e.g., shiny or transparent) reflect light in ways the algorithm cannot process. Capturing complex objects may require manual adjustment for hidden areas. Despite camera setting adjustments, photogrammetry limitations can lead to errors, necessitating post-reconstruction checks to refine results. Non-Lambertian surfaces should be coated with reflective materials like paint or tape, and featureless areas on the model should be textured to enhance reconstruction accuracy.

### 3. CASE STUDIES AND WORKING

#### 3.1 Product development of gear rod knob

Physical prototyping is an important part of product development, providing tangible models to bring design concepts to life and improve communication. A notable approach to physical prototyping, clay modelling uses clay as the primary material to form prototypes, giving designers the flexibility to modify and improve them by hand. This hands-on experience allows exploration of form, ergonomics, and aesthetics, facilitates rapid iteration, and fosters creativity. Clay modelling is especially valuable in the early stages of product development, allowing designers to test and validate ideas before moving on to advanced prototyping techniques. The flexibility and malleability of clay allows designers to intuitively experiment and rapidly generate and modify shapes while gaining a deeper understanding of the physicality of the product. This iterative design process is supported by clay modelling, which facilitates rapid adjustment of proportions, surface details, and overall aesthetics in real time, fostering creativity and problem-solving. Clay modelling evokes multiple senses and enhances the creative process by allowing designers to feel the texture, weight, and contours of the clay, leading to deeper insight and design refinement. In terms of cost and time efficiency, clay modelling can prove advantageous as it is relatively cheap, readily available, and requires minimal equipment. It is especially useful when exploring concepts, as changes can be implemented in the field without complex tools. Clay models serve as excellent collaboration tools for interdisciplinary teams, providing concrete reference points for collaborative discussion and feedback. Stakeholders can actively participate in meaningful discussions about product design and foster effective communication and coordination among team members. Additionally, clay models evoke emotional responses, creating excitement, curiosity, and connection. This emotional connection helps assess a product's appeal and potential market acceptance. Despite its advantages, clay modelling has the following limitations, suitable for complex shapes or precise measurements. Therefore, comprehensive product development may require combining clay modelling with other prototyping techniques such as digital modelling and 3D printing. In summary, clay modelling is a valuable technique in physical prototyping that enables tactile and intuitive exploration, rapid iteration, cost efficiency, collaboration, and emotional engagement. This is illustrated in a case study where clay modelling was used to create a reference model of a precisely fitted gear knob. The design data captured by photogrammetry was iteratively modified using CAD software to optimize the clay model and demonstrate the reverse engineering process in prototyping.



The above figures (i-vii) show the design of gear rod knob which physically prototyped by using clay modelling and CAD modelled from the reference model of an original gear rod knob of a Maruthi 800 and the output model is created by using the factors like flexibility and physical engagement in use of the gear rod knob in satisfactory condition and it is shown figure (vii) in the 3D printing preview interface and slicer with software ultimaker CURA. This process results the advancements of design iteration conditions in product development.

### 3.2 Design modification of security camera support

Design is the process of creating a plan or blueprint for building an object or system with the aim of achieving specific goals or requirements. It is a creative process of identifying needs, considering solutions, and making decisions about the best way to achieve desired results. Design can be applied to a variety of fields, including engineering, architecture, graphic design, and product design. A combination of technical skills and creative thinking is required, as designers must consider factors such as functionality, aesthetics, ease of use, and cost when creating designs. The design process typically includes several phases: research and analysis, conceptualization, prototyping, testing, and refinement . Effective design requires a deep understanding of the problem at hand and the ability to generate and evaluate multiple possible solutions to arrive at the best possible design. The support stand, one of the components that makes up the body, serves as the basic base for the camera body, as well as a mounting base for other important components such as support screws and clamps. Design data is extracted using a light scanner to collect the model design for the sparse cloud point model. Figure 1 below shows the structure of the optical scanner.



Figure 1 :3D Scan setup of structure light based scanner.

Further in-depth information regarding the support stand may be found in subsequent subchapters that explore various aspects of its design, function. As a key component in the overall construction of the camera body, the support stand plays a vital role in ensuring the camera body overall functionality and durability.

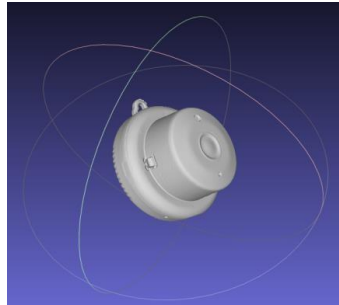


Figure 2 : 3D Scanned virtual model of the security camera is generated by using the structured light 3D scanner. The above figure 2 shows the scanned virtual model of the camera body and the designed model of the stand for camera. The design of the security camera support stand is done by the help of the required shape and style in the Autodesk fusion 360 CAD software by giving the design input dimensions in the software and creating the support design in the software and further that design is exported to the manufacturing process. The final modified model of the design is shown in figures 3 and 4.

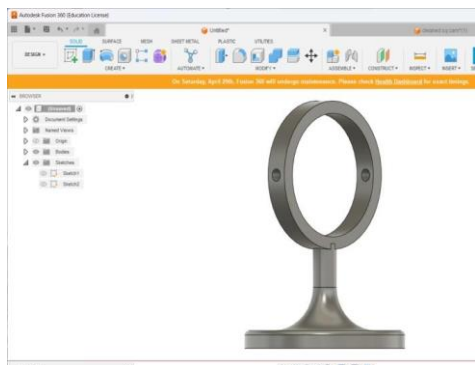


Figure 3 : Design modification for security camera support stand



Figure 4 : Assembled model of security camera (virtual camera and 3D designed support stand model).

The product development of security camera support results the process of advancement in integration of physical to digital model generation and creating the attachments to the digital model by integrating the design and analyzing the data from the digitized model using the 3D scanning technology in the software and reducing the production for testing the design model.

### 3.3 Reverse engineering of EV scooter design data

Scanning an automobile using photogrammetry involves capturing a series of photographs from various angles to create a detailed 3D model of the vehicle. Photogrammetry utilizes computer vision algorithms to analyse the images, identify common points, and reconstruct the geometry of the scanned object. In the case of automobiles, photogrammetry can be used to capture the exterior and interior of the vehicle, including its shape, contours, and intricate details. By employing photogrammetry, automotive designers and engineers can obtain an accurate digital representation of the automobile, which can be further utilized for various purposes. This includes virtual design modifications, visualization of different paint colours or finishes, analysis of aerodynamics, integration of new components or accessories, and even virtual reality experiences. Photogrammetry-based scanning of automobiles provides a cost-effective and efficient method for generating high-quality 3D models that can support design, marketing, and production processes in the automotive industry.

The below figures 5 and 6 shows working and extraction of physical model data to the digital model creation by using the both hardware and software as digital model generation factors, similarly other figures 7 - 19 shows the 3D scanned model is joined together to form a single design model or body then it is saved into the the design support file which is used for future upgradation in design changes and modifications.



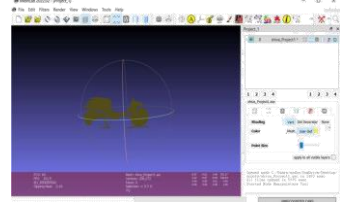
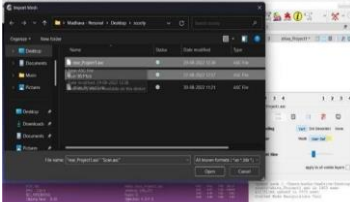
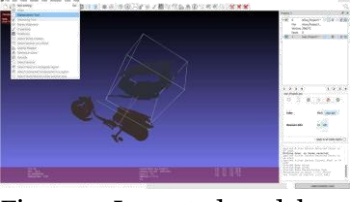
Figure 5 : 3D scanning operation by using the structured light scanner and photogrammetry process.



Figures 6 : 3D generated virtual data of scanned automobile in different views.

### 3.3.1 Editing the scanned model

The scanned model is in the format of digital model which is called as point cloud model and it is exported as stl file and the stl file is exported to the siemens NX software and in the software the design is imported and then it is exported to the part model (.prt). The converted part model is then used for editing for design modification and design improvements are given below figures 14 – 19 shows the editing process in the meshlab software.

 <p>Figure 7: Importing the scanned model to the software</p>	 <p>Figure 8: Imported model as part-1</p>	 <p>Figure 9: Imported model as part-2</p>
--	---	--

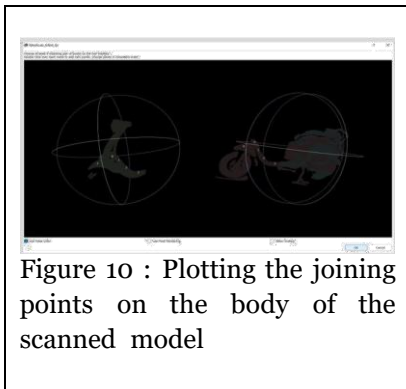


Figure 10 : Plotting the joining points on the body of the scanned model

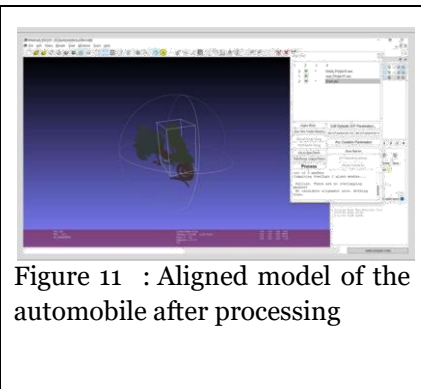


Figure 11 : Aligned model of the automobile after processing

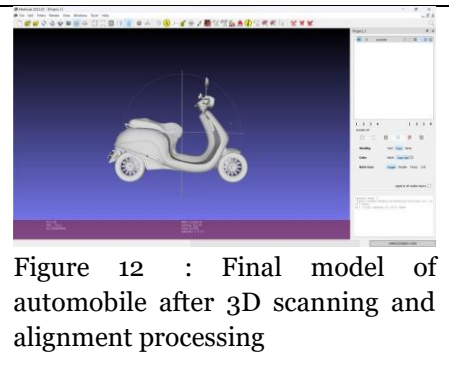


Figure 12 : Final model of automobile after 3D scanning and alignment processing

### 3.4 DESIGN AND ANALYSIS OF SUSPENSION SYSTEM

A suspension system, usually referred to as a shock absorber, is a mechanical component used in automobiles to reduce the impact of bumps and rough terrain when driving. Vehicles with shock absorbers provide a more comfortable ride. Without them, the ride would be bouncy, and the automobile shaking would be as severe as the road's unevenness. Twin shock absorbers at the rear served as the main suspension component on two-wheelers (motorcycles) in the past. However, there were substantial improvements in rear suspension design between the 1970s and the 1980s. As a result, single rear suspension systems were adopted widely and started to become the standard. Twin shock absorbers were primarily found on historic motorcycles as they became less popular. They gradually made their way into inexpensive cars and are now more frequently used. The main purpose of the suspension system on a two-wheeler is to shield the driver and the vehicle from the impact of the uneven road surface. When supported by weight, an effective suspension system should move as little as possible, be inexpensive, light, and require little upkeep. working of two-wheeler suspension system: The two main parts of a two-wheeler's suspension system are: Helical coil spring, Hydraulic damper with a piston setup. Both components work together to ensure a smooth and comfortable ride for the rider. A helical coil spring is a flexible material formed into a spiral shape by twisting a wire. It changes its shape when pressure is applied along its axis. The use of these springs allows the vehicle's main body to move independently from the tyres. This means that the vehicle's main structure doesn't follow the up and down motion of the tires when traveling on rough surfaces. A damper, on the other hand, absorbs the impact that the spring experiences and slows down the spring's movement. This damping effect happens using hydraulic fluid. A piston moves back and forth inside a cylinder filled with this fluid. The energy produced by the spring's motion is turned into heat energy by the damper. This heat is then released into the surroundings. This process reduces the impact of bumps and results in a more comfortable ride for the rider. The figures 13- 15 shows the working of 3D scanned model in the CAD and analysis software.

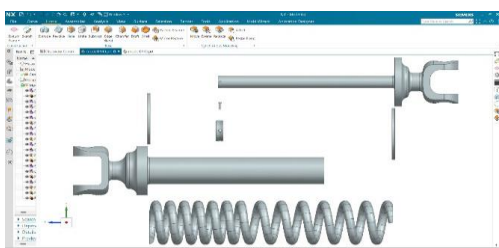


Figure 13 : Mono pre-assembly

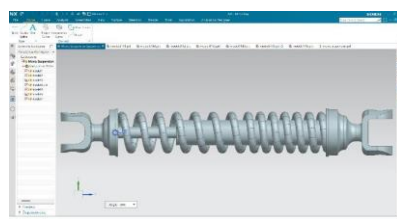


Figure 14 : Mono assembly

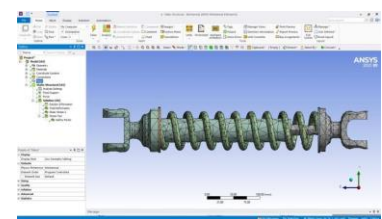


Figure 15 : Mono meshing

#### 3.4.1 Specification of problem

Research and studies from the past have shown that a variety of materials are used in the fabrication of springs for two-wheeler shock absorbers and suspension systems both in India and around the world. The best materials for making these springs have been the subject of various investigations, with variable degrees of success.

Eight of these resources were chosen for this study's in-depth research. Based on conclusions gathered from many other research articles, these materials have been identified as top competitors for fabricating springs in two-wheeler shock absorbers. The goal of the research is to choose the best material out of these 8 possibilities. This will be accomplished by contrasting the deformations and stresses that each material displays under particular circumstances.

3.4.2 Dimensions of two-wheeler suspension system model:

Parameter	Value	Description
Mean diameter of coil (D)	82 mm	Average diameter of the helical spring coil.
Diameter of wire (d)	11 mm	Diameter of the wire used to form the spring.
Total number of turns	16	Total number of complete turns of the coil.
Outer diameter of spring coil (Do)	93 mm	Maximum outer diameter of the spring coil.
Spring index (C)	7.45	Ratio of mean coil diameter (D) to wire diameter (d).
Loads Used for Analysis		
Weight of bike	118 kg	Weight of the bike alone in kilograms.
Weight of one person	76 kg	Standard weight of one person typically considered in the analysis.
Weight of two persons	152 kg	Combined weight of two persons.
Weight of three persons	228 kg	Combined weight of three persons.
Weight of bike and one person	194 kg	Total weight of the bike and one person together.
Weight of bike and two persons	270 kg	Total weight of the bike and two persons together.
Weight of bike and three persons	346 kg	Total weight of the bike and three persons together.
Loads (L)		
L1	1156.4 N	Load corresponding to the weight of the bike (118 kg) in Newtons (N).
L2	1903.14 N	Load corresponding to the weight of the bike and one person (194 kg) in Newtons (N).
L3	2648.7 N	Load corresponding to the weight of the bike and two persons (270 kg) in Newtons (N)

Wahl's Stress Factor (Kw): 1.89

This table and description provide a structured overview of the dimensions, loads, and factors relevant to the helical spring under consideration.

3.4.3 Material properties: Table 2 :Materials used for analysis of suspension system

Materials	Mechanical properties					
	Density (kg/m <sup>3</sup> )	Poisson's Ratio	Young's modulus (Gpa)	Modulus of rigidity (Gpa)	Tensile strength (MPa)	Compressive strength (MPa)
Chrome vanadium steel	7800	0.27	210	80	900	1550
Chromium silicon steel	7850	0.30	200	75	1100	1700



High carbon steel	7850	0.29	210	80	550	600
Silicon manganese steel	7800	0.30	210	80	1000	2000
Aluminium alloy	2700	0.33	70	26	240	240
Carbon steel	7850	0.29	210	80	250	460
Stainless steel	8000	0.30	200	77	215	510
Music wire	7830	0.30	220	86	1000	1000

3.4.4 Simulated results of suspension system

Table 3. Results in ANSYS with respect to material and loads

Loads/ materials	Simulation values	Aluminum alloy and +				
		Chrome vanadium	Chrome silicon steel	High carbon steel	Silicon manganese steel	Music wire
L <sub>1</sub> = 1156.4 N	Deformation(mm)	0.111	0.123	0.115	0.117	0.112
	Stress (MPa)	425.67	424.37	424.87	423.99	424.47
	strain	0.0041	0.0041	0.0041	0.0041	0.0041
L <sub>2</sub> =1903.14N	Deformation(mm)	0.183	0.202	0.190	0.193	0.185
	Stress (MPa)	699.84	697.69	698.52	697.77	697.85
	strain	0.0068	0.0068	0.0068	0.0068	0.0068
L <sub>3</sub> = 2648.7 N	Deformation (mm)	0.255	0.282	0.264	0.269	0.257
	Stress(MPa)	974	971.01	972.17	971.13	971.24
	strain	0.0094	0.0095	0.0095	0.0095	0.0094

Table 4. Results in ANSYS with respect to material and loads

Loads/ materials	simulation values	Carbon steel +				
		Chrome vanadium	Chrome silicon steel	High carbon steel	Silicon manganese steel	Music wire
L <sub>1</sub> = 1156.4 N	Deformation(mm)	0.066	0.069	0.066	0.066	0.087
	Stress (MPa)	424.54	423.37	423.81	422.96	422.62
	strain	0.0024	0.0025	0.0024	0.0024	0.0023
L <sub>2</sub> =1903.14N	Deformation(mm)	0.108	0.114	0.109	0.109	0.144
	Stress (MPa)	697.98	696.06	696.7	696.08	695.53
	strain	0.0040	0.0042	0.0040	0.0040	0.0038
L <sub>3</sub> = 2648.7 N	Deformation (mm)	0.151	0.159	0.152	0.152	0.200
	Stress(MPa)	971.42	968.48	969.74	968.77	968
	strain	0.0056	0.0051	0.0055	0.0055	0.0053

Table 5. Results in ANSYS with respect to material and loads

Loads/ materials	Simulation values	Stainless steel and				
		Chrome vanadium	Chrome silicon steel	High carbon steel	Silicon manganese steel	Music wire

L <sub>1</sub> = 1156.4 N	Deformation(mm)	0.086	0.070	0.090	0.091	0.087
	Stress (MPa)	424.29	423.38	423.49	422.61	422.64
	strain	0.0024	0.0025	0.0024	0.002	0.0023
L <sub>2</sub> =1903.14N	Deformation(mm)	0.142	0.115	0.147	0.150	0.144
	Stress (MPa)	697.56	696.07	696.25	695.51	695.56
	strain	0.0040	0.0042	0.0040	0.004	0.0038
L <sub>3</sub> = 2648.7 N	Deformation (mm)	0.197	0.160	0.205	0.210	0.200
	Stress (MPa)	970.83	968.75	969.01	967.98	968.04
	strain	0.0056	0.0058	0.0055	0.0055	0.0053

### 3.4.5 Cost Analysis for Suspension System:

The cost analysis for the suspension system components shows that Chrome Silicon Steel, priced at ₹600 per kg, and Aluminium Alloy, costing ₹300 per kg, are the primary material costs. Direct labor is ₹350 per unit for one hour, while direct manufacturing expenses amount to ₹150 per unit. Overhead costs include ₹150 for rent (monthly rent divided by 10 units) and ₹75 for utilities (monthly utilities divided by 10 units). Equipment depreciation adds ₹100 per unit, and administrative costs are ₹50 per unit. Combining these costs, the total manufacturing cost per unit is ₹1625. Adding marketing expenses of ₹100 per unit and distribution costs of ₹50 per unit, the total production cost per unit becomes ₹1775. With a 15% profit margin applied to the total production cost per unit, the profit margin amounts to ₹266.65. Therefore, the selling price per unit, including the profit margin, totals ₹2041.65. This analysis underscores the significant impact of material costs, labor, overhead, and profit margin on determining the final selling price for each unit of the suspension system components.

## 4. EXPERIMENTAL RESULTS

### 4.1 Design Modification of Security Camera Stand by Using Product Development:

In first case the design modification is made simple and easy, so that the camera body can be adjusted according to the view angle and the design of the camera is modified by adding the support stand to it and it can also portable and removed when there is no use. The final output can be seen by design modification is that by using the software the rapid dimensions are used to design the support stand it is manually tested in the software by adding the simulated model in the CAD model. This process enables the digital model iteration which helps in material wastage management and time consumption by 28% in production process compared to second case study. The below figure shows the intersection of simulated model to the design model.

Figure 16 : Final result of design modification of security camera stand by using product development

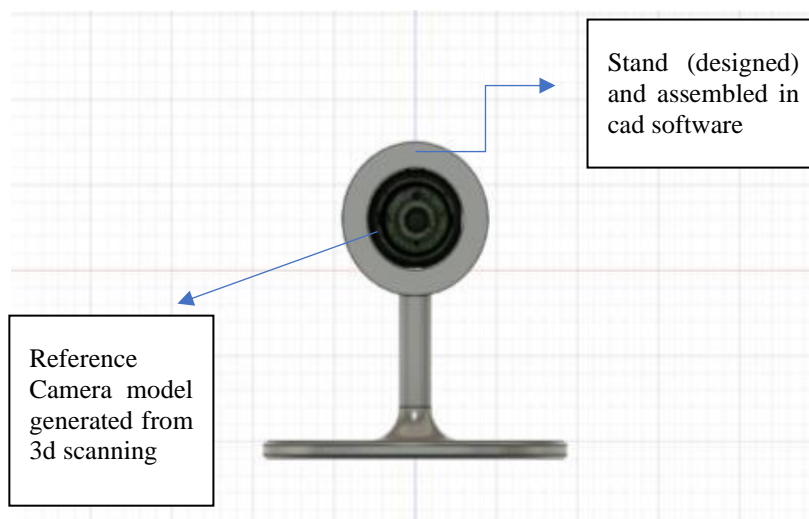


Table 8 : Steps of the 3D scanning process for security camera using product development (Photogrammetry)

Sl.no	Task	Description	Duration [min:s]
1	Scanning the security camera	Adjust the camera position and focal length before initiating the automatic capturing process.	1:35
2	Reconstruction	COLMAP is used for both sparse and dense reconstruction by first estimating camera positions and generating a sparse point cloud, and then refining the model with a detailed dense point cloud and mesh.	27:05
3	Meshlab script	Remove the dark-colored mesh using the conditional selection tool and reduce the number of faces to simplify the model.	0:07
4	Manual mesh editing	Scale the model, add thickness, smooth the surface, and then export it as an STL file.	4:20
5	Surface estimation	Apply a freeform surface fit to generate a parameterized model, achieving an average maximum error of 0.22 mm and 3.9 mm, respectively.	5:10
6	Surface extraction	Extract the camera by intersecting the parameterized surface with the extruded shape, then apply a thickness of 2 mm to the surface.	2:28
7	Final model	Preparing model for printing	1:00
Total/Final			42:15

Table 9 : Steps of the 3D scanning process for security camera using product development (3D scanner)

Sl.no	Task	Description	Duration [min:s]
1	Scanning Security Camera	Adjust the camera position and focal length before initiating the automatic capturing process.	0:30
2	Reconstruction	Utilize COLMAP for both sparse and dense reconstruction, starting with the creation of a sparse point cloud and camera pose estimation, and progressing to the generation of a detailed dense point cloud and mesh.	12:05
3	Meshlab scripting	Remove the dark-colored mesh with the conditional selection tool and reduce the number of faces to streamline the model.	0:09
4	Manual mesh edit	Scale the model, add thickness, smooth the surface, and export it as an STL file.	2:20
5	Surface estimation process	Apply a freeform surface fit to create a parameterized model, achieving average maximum errors of 0.22 mm and 3.9 mm, respectively.	1:10
6	Surface extraction process	Extract the camera by intersecting the parameterized surface with the extruded shape, then apply a 2 mm thickness to the surface	2:18
7	Final model	Prepare the model for printing by scaling, adding necessary thickness, smoothing surfaces, and exporting it in a suitable format such as STL.	1:00

Total/Final	20:28
-------------	-------

**4.2 Physical Prototyping Of The Gear Rod Knob Using Reverse Engineering:**

In first case the physical prototyping is used for simple and user satisfactory as the theme for product development of the gear rod knob as a model, the design is extracted from the original model and reflected the changes by using the clay modelling as the prototyping process and after making the prototype model that model is scanned for digital twin which is used for future usage and it helps in storing the design model as digital model, the digital model is used as a reference model for design modification and by that model we can create the optimized models by using the CAD software. The result helped design modification process in product development, customizing gear rod knobs resulted improvement in design iterations and user need by both traditional and non-traditional product development process with respect to time consumption by 22% and the result which helped greatly in enhancing the user experience in product development. The below figure shows case two process.

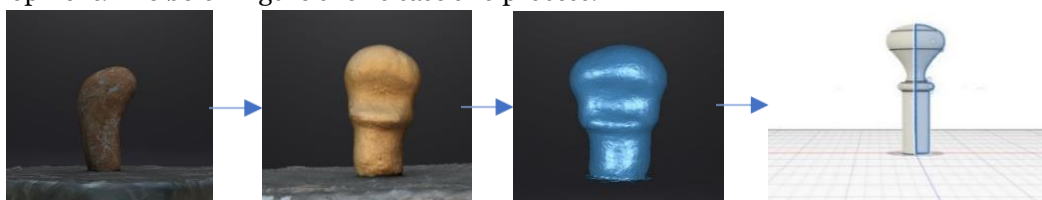


Figure 17 : Final result of physical prototyping of the gear rod knob by using reverse engineering

Table 6 : Steps of the 3D scanning process for physical prototyping of gear rod knob using reverse engineering (3D scanning)

Sl.no	Task	Description	Duration [Second]
1	Clay shapping and scanning	Mixing three different colors of soft clay, then shaping and fitting the clay before starting the scan.	6:14
2	Reconstruction	Generating a sparse point cloud with COLMAP, then a dense point cloud and a refined mesh with openMVS.	2:58
3	Mesh editing and refinement	Removing the mesh generated of the clay support, closing holes and refining the mesh , before scaling the model based in a known distance.	4:43
4	Adding parametric features	Using NX to subtract the gear rod base-structure from the scanned model.	9:54
5	Final model	Preparing the model for printing	0:53
Total			24:42

Table 7 : Steps of the 3D scanning process for physical prototyping of gear rod knob using reverse engineering (photogrammetry)

Sl.no	Task	Description	Duration [Second]
1	Clay shaping and scanning	Mixing three different colors of soft clay, then shaping and fitting the clay before starting the scan.	15:03
2	Reconstruction	Generating a sparse point cloud with COLMAP, then a dense point cloud and a refined mesh with open MVS.	6:10
3	Mesh editing and refinement	Removing the mesh generated of the clay support, closing holes and refining the mesh , before scaling the model based in a known distance.	15:13

4	Adding parametric features	Using NX to subtract the gear rod base-structure from the scanned model.	13:04
5	Final model	Preparing the model for printing	0:23
Total			49:53

**4.3 Reverse Engineering of Ev Scooter Data:**

In third case study by using the reverse engineering technology the results obtained by comparison of the vehicle dimensions with the original model by using the official dimensions quote by the manufacturer as shown in below figure with the CAD dimension model in above figure, hence the prototyped model is perfectly matched the original dimensions.

Optimizing the design modification in electric scooter is extended by results 15% improvement in design validation process using the 3D scanning technology.

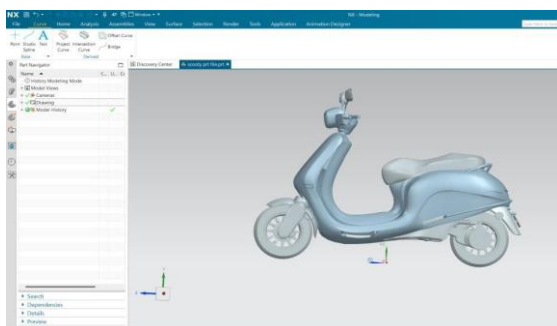


Figure 18 : Imported design view in the software interface.

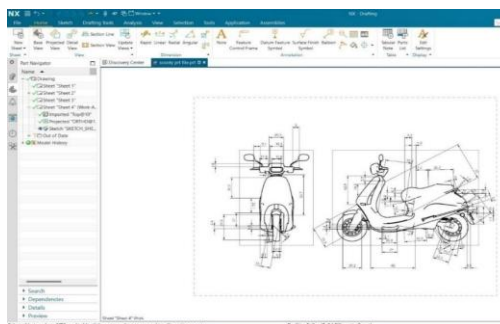


Figure 19 : Adding dimensions to the design model by using dimension tool in the software.

Table 10 : Dimensional details of EV scooter (source from <https://www.pureev.in>)

Dimensions	in mm
Length	1859
Width	712
Height	1160

Table 11: Obtained dimension result of the EV scooter model.

Dimensions	in mm
Length	1854
Width	711
Height	1154

**4.4 Design and Analysis Of Suspension System:**

In fourth case study the results obtained by performing the design and analysis of the suspension system for betterment of use and cost estimation for manufacturing by application of testing and analysis of different materials in the study.

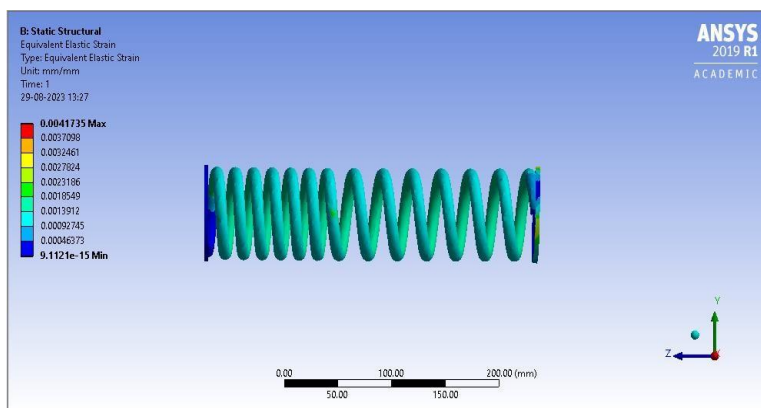


Figure 20: Analysis of suspension system

The results obtained through theoretical and simulated calculations by performing the analysis of the designed suspension system for the sustainable behaviour when subjected to different load and different material applications. The below tabular data shows the information regarding the results of the analysis.

Table 12: Theoretical and simulated results for shear stress (MPa) with respect to loads (N) for Aluminium.

Load (N)	Result (shear stress in MPa)	Simulated result of (shear stress in MPa)				
		Aluminium and				
		Chrome vanadium	Chrome silicon	High carbon	Silicon manganese	Music wire
L <sub>1</sub> = 1156.4	428.15	425.67	424.37	424.87	423.99	424.47
L <sub>2</sub> = 1903.14	704.62	699.84	697.69	698.52	697.77	697.85
L <sub>3</sub> = 2648.7	980.66	974	971.01	972.17	971.13	971.24

Table 13: Theoretical and simulated results for shear stress (MPa) with respect to loads (N) for carbon steel

Load (N)	Theoretical Result (shear stress in MPa)	Simulated result of (shear stress in MPa)				
		Carbon steel and				
		Chrome vanadium	Chrome silicon	High carbon	Silicon manganese	Music wire
L <sub>1</sub> = 1156.4	428.15	424.54	423.37	423.81	422.96	422.62
L <sub>2</sub> = 1903.14	704.62	687.98	696.06	696.76	696.08	695.53
L <sub>3</sub> = 2648.7	980.66	971.42	968.48	969.74	968.77	968

Table 14: Theoretical and simulated results for shear stress (MPa) with respect to loads (N) for stainless steel

Load (N)	Theoretical Result (shear stress in MPa)	Simulated result of (shear stress in MPa)				
		Stainless steel and				
		Chrome vanadium	Chrome silicon	High carbon	Silicon manganese	Music wire
L <sub>1</sub> = 1156.4	428.15	424.29	423.38	423.49	422.61	422.64
L <sub>2</sub> = 1903.14	704.62	697.56	696.07	696.25	695.51	695.56
L <sub>3</sub> = 2648.7	980.66	970.83	968.75	969.01	967.98	968.04

Table 15: Total cost estimation for manufacturing a suspension system.

Spring material	End support material	Total manufacturing (Rs.)	Total production (Rs.)	Target selling price (Rs.)
Chrome vanadium	Aluminium alloy	1925	2075	2321.65
	Carbon steel	1975	2125	2291.65
	Stainless steel	1905	2055	2341.65
<b>Chrome silicon steel</b>	<b>Aluminium alloy</b>	<b>1625</b>	<b>1775</b>	<b>2041.65</b>
	<b>Carbon steel</b>	<b>1675</b>	<b>1825</b>	<b>2091.65</b>
	<b>Stainless steel</b>	<b>1755</b>	<b>1905</b>	<b>2171.65</b>
High carbons steel	Aluminium alloy	1875	2025	2291.65
	Carbon steel	1925	2075	2341.65
	Stainless steel	1855	2005	2271.65
Silicon manganese steel	Aluminium alloy	1965	2115	2381.65
	Carbon steel	2015	2165	2431.65
	Stainless steel	1945	2095	2361.65

Music wire	Aluminium alloy	1895	2045	2311.65
	Carbon steel	1945	2095	2391.65
	Stainless steel	1875	2025	2291.65

The project conclude the result is chrome silicon steel(spring) and carbon steel(end support) materials are as best suspension system, compared to cost estimation analysis for all materials that are taken for analysis, the chrome silicon steel and carbon steel is best suited and has good performance where at  $L_2=1903.14$  N(simulation stress =696.06 MPa, theoretical stress =704.62MPa) similarly,  $L_3=2648.7$  N(simulation stress =968.48 MPa, theoretical stress =980.66 MPa)and which is suitable for manufacturing and cost affordability. with price range of total manufacturing price Rs.1675, total production price Rs.1825 and target selling price Rs.2091. The suspension system used in project has low total deformation andconvincing stress values which shows that the system can absorb more load and has higher strength for above specified loading conditions. Finally, the suspension system design enhanced a remarkable result by 30% reduction in production costs by adopting the importance of market survey and 20% increase in structural integrity by assigning and testing the performance of suspension system by using properties like stress, stain and deformation with different materials and loads combination in simulation.

### 5. CONCLUSION

In conclusion, this study has successfully addressed the prevalent challenge in product development by introducing a novel methodology that seamlessly transitions physical prototypes into digital models and vice versa. The utilization of accurate and cost-effective 3D scanning methods has played a pivotal role in enhancing the efficiency and cost-effectiveness of the entire product development process. The case studies presented, focusing on the modification of a security camera mount, customization of speed nodes, and optimization of electric motorbike design, demonstrate tangible benefits in terms of reduced material waste, time consumption, and improved design iterations.

The findings underscore the transformative impact of 3D scanning technology, showcasing a 22% reduction in material waste by eliminating the clay modelling and a 28% decrease in time consumption during the design iteration process for the security camera mount. Additionally, the customization of speed nodes led to a 22% reduction in time consumption, contributing significantly to enhancing user requirements and overall design iterations of gear rod knob. The optimization of electric motorbike design, facilitated by 3D scanning, resulted in a 15% improvement in the design validation process.

Notably, the study extended its impact to the suspension design domain, achieving remarkable results. By integrating market research, the production costs were reduced by an impressive 30%, while simultaneously enhancing structural integrity by 20%. The approach involved determining and testing the suspension system`s performance through the simulation of stress, strain, and deformation, considering various materials and loads.

These specific outcomes emphasize the practical significance of the research, offering valuable solutions for industry professionals and imparting crucial lessons for future product development endeavors. The seamless integration of physical and digital realms through 3D scanning technology has proven instrumental in achieving enhanced efficiency, reduced costs, and improved design outcomes, marking a noteworthy advancement in the field of product development methodologies.

### ACKNOWLEDGEMENT

The authors are thankful to the principal and management of Vasavi college of Engineering, Hyderabad, for providing the facilities and encouragement in carrying out the work.

### REFERENCES

1. Pilevari, S., & Yavari, S. (2020). Evolution of manufacturing through Industry 1.0 to 5.0. Journal of Industrial Strategic Management, Year 2020, Volume 5 (Issue 2), Pages:44-63.
2. Haleem, A, Javaid, M. (2022). 3D scanning's applications in Industry 4.0: Manufacturing, healthcare, and architecture, International journal of cognitive computing in engineering 3 , 161-171.

3. Nielsen, L. W, & Malik, A. H. (2019). Low-cost 3D scanning in smart learning factories. *Procedia manufacturing* 38,824-831.
4. Monchinger, P, Schroder, D., (2021). Automated CAD repositioning in construction using 3D scanning. January 2021,*Procedia CIRP* 100:530-535
5. Kohtala, M, Erichsen, A. (2021). Photogrammetry-based 3D scanning for early-phase product development. January 2021*Procedia CIRP* 100(3):762-767
6. Percoco, G, Lavecchia, F. (2015). 3D digitization of millimeter-scale products using photogrammetry *Procedia CIRP*, Volume 33, 2015, Pages 257-262
7. Fitzpatrick, C., Collins, S. (2020). Optimization of 3D scanning processes for rapid virtualization. *Procedia CIRP*, Volume 91, 2020, Pages 911-916
8. Baltasavias, P. (2012). Photogrammetry vs. laser scanning: A comparative study. *ISPRS Annals of the Photogrammetry, Remote Sensing and Spatial Information Sciences*, Volume I-3, 2012, XXII ISPRS Congress, 25 August – 01 September 2012, Melbourne, Australia.
9. Cignoni, P, Calleri, M.(2008). MeshLab: Processing mesh data with open-sourcesoftware. January 2008, Source DBLP.
10. Kazhdan M. (2013). Screened Poisson surface reconstruction for accurate digital modeling. *ACM Transactions on Graphics* Volume 32Issue 3Article No.: 29pp 1–13
11. ETH Zurich, Johannes Lutz Schönberger (2018). Robust 3D modeling from unstructured imagery.
12. Laff, M., Rentschler, I.(2018). Evolving roles of prototypes in diverse companies. February 2018*Journal of Mechanical Design* 140(6)
13. Christer W. Elverum, Torgeir Welo (2016). Prototyping in new product development strategies. December 2016*Procedia CIRP* 50:117-122.
14. Christer W. Elverum, Torgeir Welo (2015). Directional and incremental prototyping in high novelty product development. *Journal of Engineering and Technology Management*, Volume 38, October–December 2015, Pages 71-88.
15. Kaufman, L., Rennie, T. (2015). Single-camera photogrammetry for reverse engineering artifacts. December 2015*Procedia CIRP* 36:223-229,DOI:10.1016/j.procir.2015.01.073
16. Remondino F. (2011). Heritage recording and 3D modeling through photogrammetry and scanning. *Journals Remote Sensing* ,Volume 3, Issue 6
17. Thomas, M. A. ., Hassan, M. F. ., Wan Salim, W. S. I. ., & Osman, S. A. . (2020). Reconstruction of 3D Models in Automotive Engineering Applications Using Close- Range Photogrammetry Approach. *Journal of Advanced Research in Fluid Mechanicsand Thermal Sciences*, 61(2), 220–232.
18. Mrugalska. B, Dovramadjiev. T. (2021). Open-source systems and 3D design indental medical engineering. September 2021*Procedia Manufacturing* 54:296-301
19. Ismail, N., Taqriban, M. (2020). Expedited prosthetic socket production using photogrammetry and 3D printing. *Electronics* 2020, 9(9),1456.
20. Vozisova, A., Eroshenko, N. (2016). 3D scanning and printing in the electric power industry Conference: 2016 IEEE International Conference on Industrial Technology (ICIT), March 2016.
21. Matys, M., Krajcovic, M. (2021). Photogrammetry-based 3D modeling oftransportation vehicles. *Transportation Research Procedia* 55, (2021), 584– 591.
22. Luhmann, T. (2010). Industrial applications of close-range photogrammetry. November 2010, *ISPRS Journal of Photogrammetry and Remote Sensing* 65(6):558- 569
23. Ueda, T., Barari, A. (2020). Defective zone detection in turbine blades using 3Dscanning data. January 2020, *IFAC-Papers Online* 53(2) DOI :10531- 10535.
24. Adamova, A., Borosa, M. (2021). 3D scanning for optimized video surveillance placement. July 2021, *Transportation Research Procedia* 55:1665- 1672.
25. Kushwah, A., Parekh, A. (2020). Optimization of automobile suspension coil springs. December 2020, *Materials Today Proceedings*42(10).
26. Ram Kumar, K., Nacharaih, A. (2017). Two-wheeler spring suspension system analysis with composite materials. ISSN 2319-8885, Vol.06, Issue.26, August- 2017, Pages:5188-5207.



27. Manga Hymanjali. M. (2018). Design and analysis of shock absorbers, IJRET: International Journal of Research in Engineering and Technology, ISSN: 2319- 1163, May 2018.
28. Prince Jerome Christoper J., Pavendham R. (2018). Coil springs design for two-wheeler shock absorbers. International Research Journal of Engineering and Technology (IRJET) e-ISSN: 2395-0056, Volume: 05 Issue: 10 | Oct 2018
29. A.Chinamahammad Bhasha, N. Vijay Rami Reddy. (2017). Shock absorber design and analysis. International Research Journal of Engineering and Technology (IRJET) e-ISSN: 2395 -0056 Volume: 04 Issue: 01 | Jan -2017
30. Dishant, D., Paraminder Singh. (2017). Review of suspension systems in automotive engineering. International Research Journal of Engineering and Technology (IRJET) e-ISSN: 2395 -0056, Volume: 04 Issue: 04 | Apr -2017
31. Shubham Kadu, Kailas Gaware (2018). Advanced suspension system for two- wheelers. International Research Journal of Engineering and Technology (IRJET) e- ISSN: 2395-0056, Volume: 05 Issue: 08 | Aug 2018
32. Vidya S. Visave, J.R. Mahajan, (2020). Experimental investigation of mono suspension springs. International Research Journal of Engineering and Technology (IRJET) e-ISSN: 2395-0056, Volume: 05 Issue: 01 | Jan-2018
33. Bhanu Prakash Bhavare, Pratesh Jayaswal. (2021). Two-wheeler suspension system design and analysis using ANSYS. International Research Journal of Engineering and Technology (IRJET) e-ISSN: 2395-0056, Volume: 08 Issue: 05 | May2021
34. Raviraj N. Rathod, Milind S. Bodkhe. (2018). Shock absorber coil spring design and analysis for two-wheelers. International Research Journal of Engineering and Technology (IRJET) e-ISSN: 2395-0056, Volume: 05 Issue: 10 | Oct 2018 .